Malaysian Journal of Analytical Sciences (MJAS)
Published by Malaysian Analytical Sciences Society

EFFECT OF pH IN THE SYNTHESIS OF GOLD-COPPER NANOPARTICLES SUPPORTED ON ANODIC ALUMINIUM OXIDE AS CATALYST FOR THE REDUCTION OF *p*-NITROPHENOL

(Kesan pH dalam Sintesis Emas-Kuprum (Au-Cu) Partikel Nano Disokong pada Anodik Aluminium Oksida Sebagai Mangkin bagi Penurunan *p*-Nitrofenol)

Norizwan Nordin[1], Hanani Yazid[1,2], Nor Azira Irma Muhammad[2], Abdul Mutalib Md Jani[3]*

[1]Faculty of Applied Sciences,
Universiti Teknologi MARA, 40450 Shah Alam, Selangor, Malaysia
[2]Faculty of Applied Sciences,
Universiti Teknologi MARA, Perlis Branch, Arau Campus, 02600 Arau, Perlis, Malaysia
[3]Faculty of Applied Sciences,
Universiti Teknologi MARA, Perak Branch, Tapah Campus, 35400 Tapah Road, Perak, Malaysia

**Corresponding author: abdmutalib@uitm.edu.my*

Received: 9 December 2021; Accepted: 6 March 2022; Published: 27 June 2022

Abstract

Gold–copper (Au–Cu) bimetallic catalysts were prepared through chemical reduction with Cu and Au precursors at the pH of 3, 5, 7 and 9 and hexadecylamine as the capping agent to produce Au–Cu bimetallic nanoparticles (Au–Cu NPs). The colloidal Au–Cu NPs were then grafted onto an anodic aluminium oxide (AAO) support through spin coating. The AAO support was fabricated via a two-step anodization method at 80 V by using oxalic acid as the electrolyte. The Au–Cu/AAO catalysts were characterized through field emission scanning electron microscopy–energy dispersive X-ray spectroscopy, Fourier transform infrared spectroscopy and inductive coupled plasma–optical emission spectroscopy. The catalytic activities of the Au–Cu bimetallic catalysts in the reduction of *p*-nitrophenol (*p*-NP) were evaluated. Results showed that the rate constant (k) varied in accordance with the pH of the Au precursor. The highest k value of 4.6×10^{-3} s^{-1} was obtained with the Au–Cu catalyst prepared at pH 7. The better performance of the investigated bimetallic catalyst than that of the monometallic Au and Cu catalysts demonstrated the promotional role of the second metal in the reduction of *p*-NP.

Keywords: Au–Cu NPs, pH, anodic aluminium oxide

Abstrak

Pemangkin dwilogam Au-Cu dengan prekursor Au pH 3, 5, 7 dan 9 disediakan dengan menggunakan prekursor Cu secara kaedah penurunan kimia dengan heksadesilamin (HDA) sebagai agen penutup untuk penghasilan nanopartikel Au-Cu (NP Au-Cu). Dwilogam NP Au-Cu telah dicantumkan pada sokongan anodik aluminium oxida (AAO) melalui kaedah salutan putaran. Sokongan AAO telah difabrikasi pada 80 V menggunakan asid oksalik sebagai elektrolit melalui kaedah anodisasi dua langkah. Pemangkin Au-Cu/AAO dicirikan oleh mikroskopi elektron pengimbasan pelepasan medan-spektroskopi sinar-X penyerakan tenaga (FESEM-EDX), spektroskopi inframerah transformasi fourier (FTIR) dan spektroskopi pelepasan plasma-optik berganding induktif (ICP-OES). Penurunan *p*-nitrofenol digunakan untuk menilai aktiviti pemangkin bimetal Au-Cu. Keputusan

menunjukkan bahawa pemalar kadar, (*k*) adalah berbeza bergantung kepada pH prekursor. Nilai *k* tertinggi iaitu 4.6 x 10^{-3} s^{-1} telah diperolehi daripada pemangkin Au-Cu yang disediakan pada pH 7. Daripada kajian ini, pemangkin dwilogam menunjukkan prestasi yang lebih baik berbanding pemangkin Au dan Cu logam mono, menunjukkan peranan promosi logam kedua ke arah penurunan *p*-nitrophenol.

Kata kunci: NP Au-Cu, pH, anodik aluminium oksida

Introduction

Gold nanoparticles (Au NPs) are small particles with diameters that range from 1 nm to 100 nm and unique optical and electronic properties. Au NPs can be easily dispersed in water to form colloidal Au, which offers many benefits for various applications. Au NPs are an excellent catalyst for the selective oxidation or hydrogenation of organic substrates. In recent years, interest in using Au NPs as catalysts for the reduction of p-nitrophenol (*p*-NP) and p-nitroaniline (*p*-NA) has grown [1-2]. Au NPs have been extensively researched as monometallic or bimetallic NPs. The performance of monometallic Au NPs is limited by particle size and manufacturing technique, but these constraints can be overcome by adding a second metal [3-6]. Au NPs mixed with other transition metals such Au-Pt, Au-Cu, Au-Pd, and Au-Ag have higher catalytic activity than monometallic Au NPs. It is highlighted that Au-Cu NPs are an excellent bimetallic alloy because they are more resistant to oxidation thus have a longer catalytic lifetime [5]. The characteristic of the NPs is highly dependent on their preparation condition such as pH, capping agent and precursor concentration.

However, the Au-Cu NPs tend to agglomerate on their own [6-15]. This can be prevented by introducing the support materials such as metal oxides to stabilize and disperse the Au-Cu NPs. Anodic aluminium oxide (AAO) was chosen as the support as it offers several advantages, such as (i) high surface area and porous structure; the reactants get easy access to the active catalytic site [16-17], (ii) prevent agglomeration of Au-Cu NPs, and (iii) this supported catalyst can easily be separated from the reaction mixture at the end of the reaction by simple filtration.

p-NP is a common pollutant that originates from agricultural, pharmaceutical and petrochemical industries; it is highly carcinogenic and tends to persist in water and soil [2,18]. *p*-NP causes the irritation and inflammation of the eyes, skin and respiratory tract. The delayed reaction of *p*-NP in the blood of people exposed to this compound causes methemoglobinemia. The symptoms of methemoglobinemia include cyanosis, confusion and unconsciousness. Therefore, this compound has prompted the development of a wide range of analytical devices by researchers for its determination and eventual removal from contaminated sites. The reduction of *p*-NP can be monitored easily by using a UV-Vis spectrophotometer at 400 nm. Therefore, in this work, we proposed the preparation of Au–Cu NPs with a Au precursor at different pH values via chemical reduction followed by immobilization on an AAO membrane through spin coating. The activities of these Au–Cu/AAO catalysts were then tested in *p*-NP reduction. *p*-NP is a pollutant that is commonly found in most water bodies; it can be upcycled for use in the production of analgesics, such as paracetamol, through reduction into p-aminophenol [1,6].

Materials and Methods

Preparation of Au-Cu NPs

The bimetallic Au-Cu NPs were synthesized based on the chemical reduction technique. An aqueous solution of $CuCl_2 \cdot 2H_2O$ (50 mM) was mixed with 0.3 mL $HAuCl_4 \cdot 3H_2O$ (50 mM) of various pH of 3, 5, 7, and 9 by using 0.5 M NaOH. The molar ratio of the Au to Cu is 2.5 to 1. The mixture was then added with 0.28 mL of glucose (0.5 M) in a glass vial containing the hexadecylamine (HDA) solution of 22.5 mg in 2 mL distilled water [3]. The vial was magnetically stirred at room temperature overnight followed by heating treatment at 100 ^{o}C for 10 mins. After the vial was cooled in an ice bath, 15 mg of HDA was added and the vial was heated again till colour changes observed.

The samples are denoted as Au-Cu pH3, Au-Cu pH5, Au-Cu pH7 and Au-Cu pH9.

Fabrication of AAO membrane

A 99.99% purity aluminium foil with a thickness of approximately 0.1 mm was cut into (2 cm x 2 cm) pieces, and an AAO membrane was formed on the aluminium foil using a two-step electrochemical anodization procedure that was previously reported [1,16]. The AAO was manufactured in multiple phases. The aluminium foils were cleaned and degreased in the first phase by sonication in acetone for 15 mins. The aluminium foils were then submerged in a chemical polishing solution (15 mL HNO_3 and 85 mL H_3PO_4) for 1 min at 70 °C. Then, using 0.3 M oxalic acid as the electrolyte, the initial anodization was performed for 1 minute at 5 °C with a constant voltage of 80 V. The anodic layer was then removed by immersing the foil for roughly 2 hours in a solution of 1.5 wt.% chromic and 6 wt% phosphoric acids. Next, the second anodization procedure was carried out for 2 hours in the conditions described above. Finally, a solution of 5% $CuCl_2.2H_2O$ and 15% HCl was used to dissolve the aluminium foils and obtain AAO membrane. The constructed AAO membrane was cleaned multiple times with generous volumes of ethanol and DI water and stored in the desiccator until further used.

Immobilization of Au-Cu NPs on AAO

The previously prepared Au-Cu NPs solution was deposited on both sides of the AAO by spin-coating at 1000 rpm for 30 s. Subsequently, the AAO was subjected to calcination at 400 °C for 4 hours at a rate of 10 °C/min. The immobilized Au-Cu NPs are denoted as Au-Cu/AAO pH3, Au-Cu/AAO pH 5, Au-Cu/AAO pH 7 and Au-Cu/AAO pH 9 correspond to the Au-Cu NPs prepared at pH 3, 5, 7, and 9, respectively.

Reduction of *p*-Nitrophenol

The *p*-NP solution was prepared by dissolving solid by *p*-NP (99%, Sigma Aldrich) in distilled water. In a cuvette, 1 mg of Au-Cu/AAO catalyst was added to a solution of $NaBH_4$ (1.5×10^{-2} M, 1.5 mL) and *p*-NP (0.05×10^{-2} M, 1.5 mL). The absorbance of the *p*-NP solution was determined at 1-minute intervals using a UV–vis spectrophotometer (Lambda 25, Perkin Elmer) set at 399 nm. At room temperature and pressure, the catalytic reduction was carried out. Depending on the catalyst, the total reaction time for complete reduction of *p*-NP would take 5 to 10 mins. Pseudo-first-order kinetics was used to get the value of the rate constant (*k*) as described by Yazid et al. [6].

Characterization

Characterization of the catalysts by Fourier Transform Infrared Spectroscopy was used to assess the surface functionalities of the produced samples (FTIR; Spectrum, Perkin Elmer). Meanwhile, the surface morphology was observed via Field Emission Scanning Electron Microscopy (FESEM: FEI Nova Nanosem 450). The elements of Au and Cu loading on the AAO membrane were determined by using an Inductive Couple Plasma-Optical Emission Spectrometer (ICP-OES: Optima 8000, Perkin Elmer).

Results and Discussion

Immobilization of Au-Cu NPs on the AAO

Figure 1 shows the photograph of AAO and Au-Cu/AAO. The change of color from yellow to light purple indicates the successful deposition of Au on AAO. The calcination process will vaporize any organic material from the previous steps and leave just the metal and metal oxide species which are Au-Cu NPs and AAO membrane. The calcination step also ensures that the Au-Cu NPs are covalently bonded to the -OH group on the AAO membrane [1,6]. This strong covalent bond prevents aggregation of the particles thus improving their catalytic performance. The spin-coating method provides homogenous distribution of the NPs on the AAO membrane. It is to note that all catalysts prepared at pH 3 to 9 show the same appearance to the naked eyes (Figure 1).

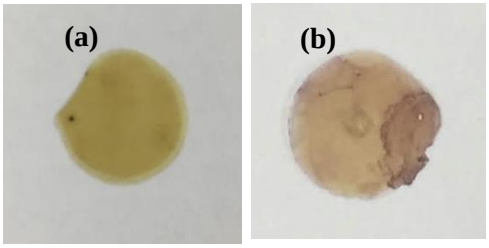

Figure 1. Photograph of (a) bare AAO (b) Au-Cu/AAO pH3

The FTIR spectra of the bare AAO (bAAO) and Au-Cu/AAO are presented in Figure 2. Some changes of peaks intensity, particularly O–H vibrations, confirm the attachment of the Au-Cu NPs on the surface of the AAO [7]. The O–H peak in bAAO at 3210 cm^{-1} is very sharp when compared to Au-Cu/AAO O-H peak at 3195 cm^{-1}. Even though the FTIR instrumentation was unable to detect the presence of gold and copper in the compound, it could be inferred through the observed peak shifting for O-H from 3210 cm^{-1} to 3195 cm^{-1}.

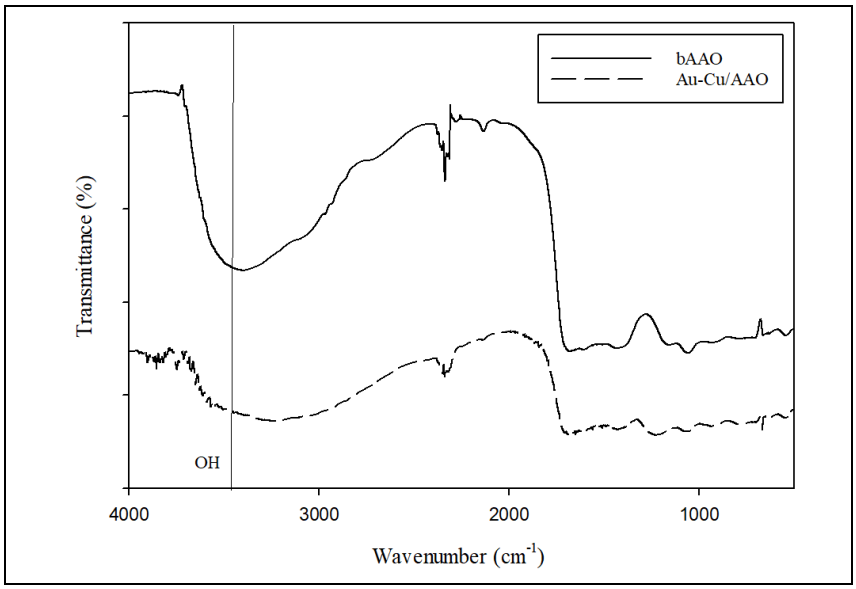

Figure 2. FTIR spectra of bAAO and Au-Cu/AAO

Figure 3 shows FESEM images of synthesized Au-Cu/AAO at pH3 to pH9. FESEM images taken from the top indicated the creation of a hexagonally aligned AAO structure via electrochemical anodization, with typical pore sizes of 100-110 nm. The pores are non-intercrossing and cylindrical in shape resulting in a high surface area. The nanostructure of the as-prepared AAO has a considerable effect on the accessibility (flow) of liquid reactants on both sites of the porous support. A good flow for the reactant to reach the active site is vital for efficient catalytic performance. It is worth noting that exact control of the AAO structure's size and interpore spacing may be accomplished by adjusting the anodization conditions and electrolyte concentration, respectively [16].

The adjustment of pH of the Au precursor has resulted in different sizes and arrangements of the NPs. On Au-Cu/AAO pH3 the size of the NPs is between 113.75 ± 85.20 nm and the NPs are clustered together as shown in Figure 3(a). Whereas, Au-Cu/AAO pH5 and pH7 demonstrated a mix of clustered and individual arrangement of the NPs with a size of 61.54 ± 96.55 nm and 32.33 ± 22.75 nm, respectively. An individually disperse NPs was shown by Au-Cu/AAO pH9 with a size of 34.33 ± 56.47 nm. Noting that the adjustment of pH of the precursor will result in various arrangement and sizes. Table 1 summarizes the characteristic of Au-Cu NPs as observed from FESEM images.

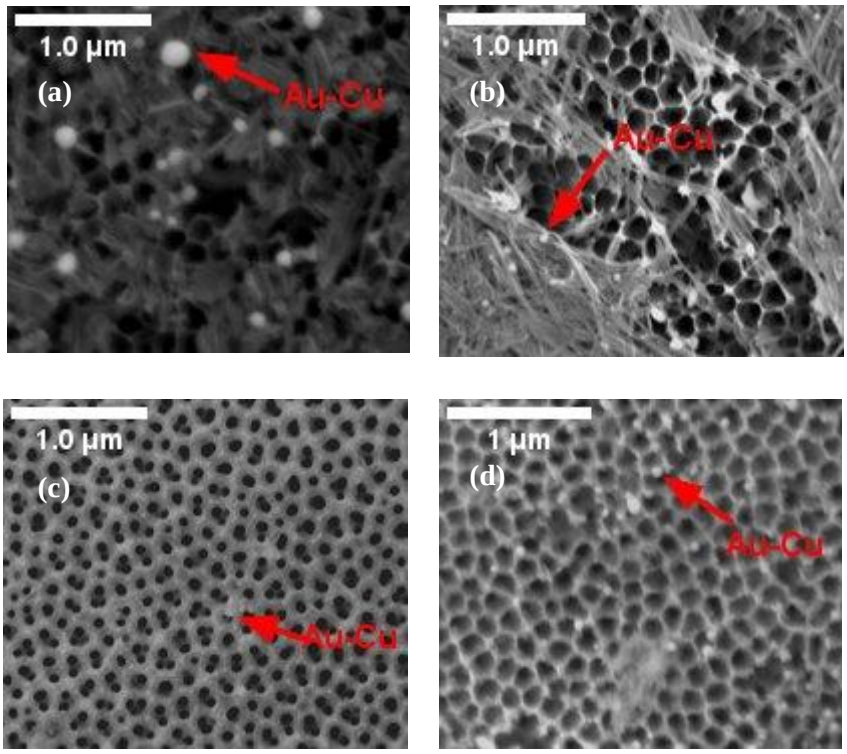

Figure 3. FESEM images of Au-Cu/AAO at different pH of (a) 3 (b) 5 (c) 7 and (d) 9

Table 1. Summary of the characteristic of Au-Cu NPs observed from FESEM images

Catalyst	Diameter Size (nm)	Distribution
Au-Cu/AAO pH3	113.75 ± 85.20	Clustered
Au-Cu/AAO pH5	61.54 ± 96.55	Mix of Clustered and Individual Dispersal
Au-Cu/AAO pH7	32.33 ± 22.75	Mix of Clustered and Individual Dispersal
Au-Cu/AAO pH9	34.33 ± 56.47	Individually Disperse

The Au-Cu pH 7 was selected for an area scan using EDX analysis (Figure 4). Figure 4(a) shows the area viewed using FESEM. Figure 4(b) depicts only large Au NPs can be detected. Small Au NPs and Cu NPs were also present but cannot be monitored clearly as seen in Figure 4(b) and (c). In contrast, the Al species from the support AAO can be seen clearly. The production of small and highly dispersed NPs on the AAO membrane resulted in reading below the EDX detection limit for small Au and Cu species. The presence of Cu species will be proved when using ICP-OES.

Based on the ICP-OES results presented in Figure 5, the Au to Cu molar ratio were determined to be 1.4: 1, 1.7:1, 2.27:1 and 1.59:1 for the Au-Cu/AAO pH3, pH5, pH7 and pH9 samples, respectively. The Au-Cu/AAO pH 7 is the closest mol to mol ratio from the experimental value of the precursor used which is 2.5 Au to 1 Cu. These results suggest that the deprotonation of the hydroxyl groups at high pH leads to the accumulation of negative charge on the surface of the Au NPs [1,18].

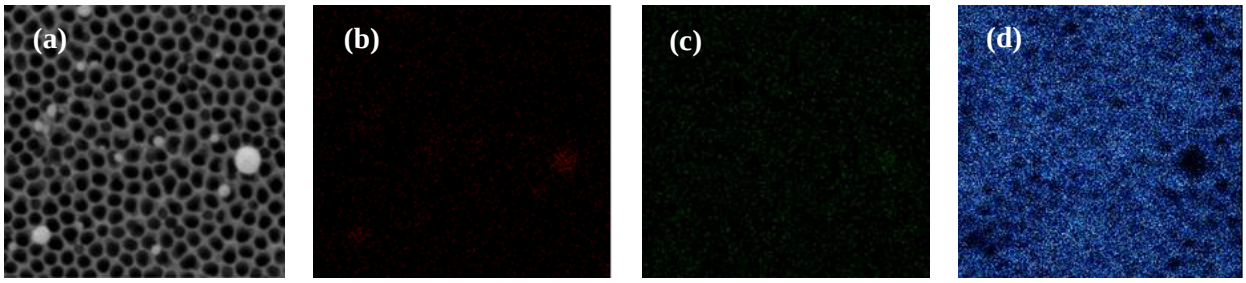

Figure 4. The Au-Cu/AAO pH 7(a) FESEM image and corresponding elemental EDX mapping of (b) Au (c) Cu and (d) Al

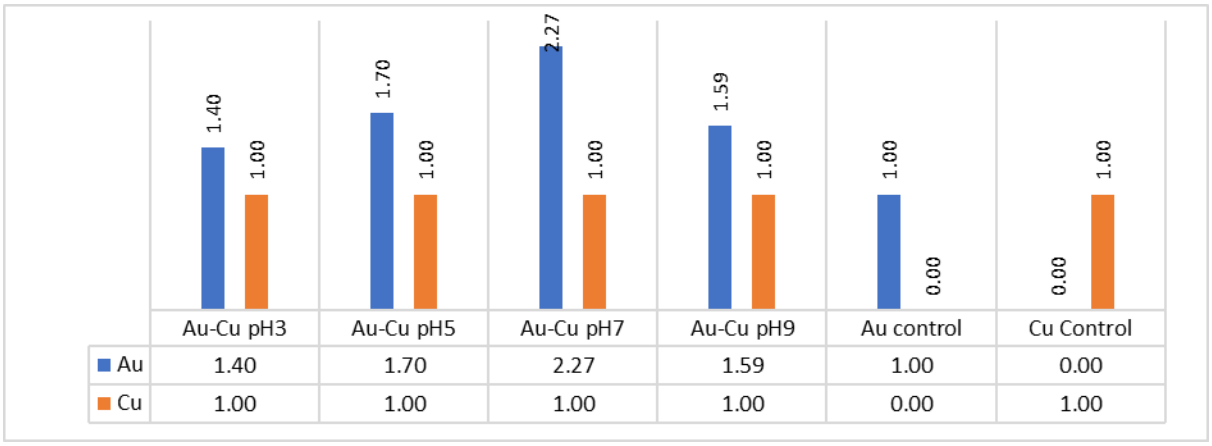

	Au-Cu pH3	Au-Cu pH5	Au-Cu pH7	Au-Cu pH9	Au control	Cu Control
Au	1.40	1.70	2.27	1.59	1.00	0.00
Cu	1.00	1.00	1.00	1.00	0.00	1.00

Figure 5. ICP-OES detection of Au to Cu molar ratio

Catalytic performance

The efficacy of the prepared Au-Cu/AAO catalysts were tested by catalytic reduction of *p*-NP to *p*-AP. The *p*-NP solution exhibited a high absorption peak at 317 nm under neutral or acidic conditions, but the addition of $NaBH_4$ increased the alkalinity of the solution, resulting in the creation of *p*-nitrophenolate ions and shifting the absorption peak to 400 nm [2,6]. The appearance and growth of a new peak at 300 nm corresponds to the formation of the product *p*-AP as shown in Figure 6 [1, 6, 18]. The gradual decrease in absorbance at 399 nm with time indicates that the nitro group has been reduced, while the appearance and growth of a new peak at 300 nm corresponds to the formation of the product *p*-AP [6,18]. The dark yellow colour of *p*-NP decreases with the formation of the *p*-AP, and bubbles are produced by $NaBH_4$ converting water to H_2 gas. Because the concentration of $NaBH_4$ in this reaction system far exceeds that of *p*-NP, its concentration remains constant throughout the reaction. The rate constant (*k*) for the reaction was calculated using pseudo-first order kinetics in the case of *p*-NP [6]. The absorbance at 400 nm remains constant over time in the absence of a catalyst, demonstrating that the reduction does not occur. Figure 6 depicts the gradual production of *p*-AP; two isosbestic spots are visible at 280 and 312 nm, implying that the conversion reaction is carried out by the two main species [1, 6].

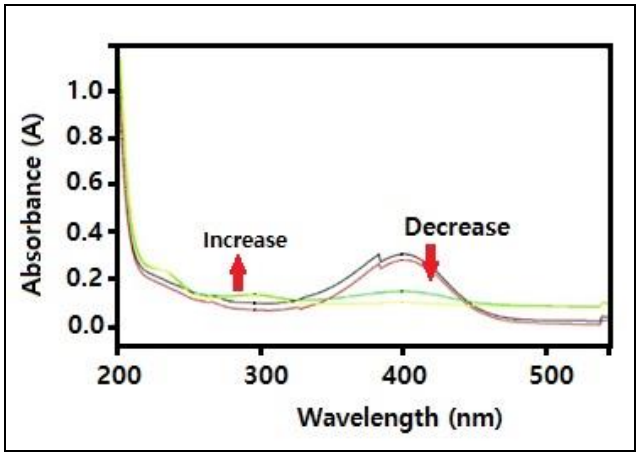

Figure 6: UV-Vis spectra of *p*-NP over time for Au-Cu/AAO pH 7

For all the studies, the graph of $\ln(C/C_o)$ vs reaction time is linear (Figure 7), showing that the catalytic reaction followed first-order kinetics. The Au-Cu/AAO pH3, pH, pH7 and pH9 samples were found to have *k* values of 4×10^{-4} s^{-1}, 2×10^{-3} s^{-1}, 4.6×10^{-3} s^{-1}, and 6×10^{-4} s^{-1}, respectively. A greater *k* value means that *p*-NP is reduced more quickly [1,6,18]. The Au control catalyst had the lowest *k* value, while Cu control had no reaction at all. These findings show that the presence of Cu had an impact in enhancing the catalytic activity of Au NPs in the reduction of *p*-NP. As previously stated, the Au-Cu/AAO pH7 catalyst possesses smaller Au NPs with a uniform distribution of clustering and individual NPs, resulting a good impact on catalytic activity. A neutral pH leads to the formation of small and a mix of individual and clustered dispersal arrangements. The various size and arrangement of Au-Cu NPs generated by grafting the NPs onto the AAO is responsible for the various *k*-values. Even though Cu shows zero catalytic activity the presence of it being with Au has increased the catalytic activity of Au when comparing Au control. Table 2 summarizes the *k*-values of all the prepared catalysts for the reduction of *p*-NP. The results indicate that the adjustment of Au precursor at pH 7 and synthesizing it with Cu has a good effect on the catalytic activity.

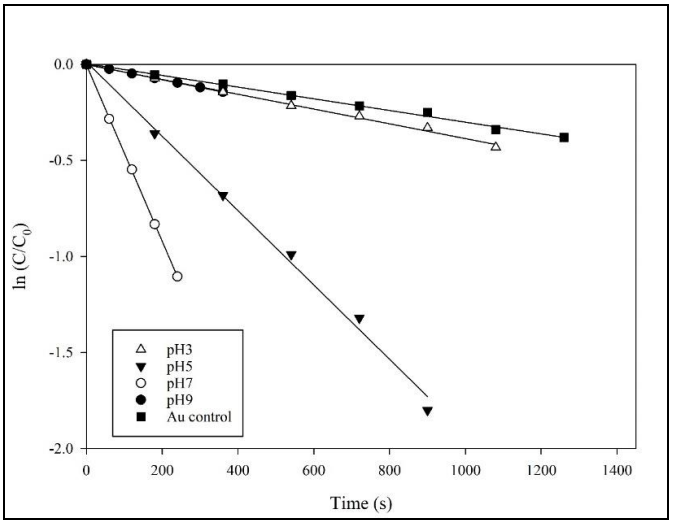

Figure 7. Plot of ln (C/C_o) versus time (min) for the catalysts Au-Cu/AAO

Table 2. Rate of reaction (*k*) of the catalysts

Catalyst	***k*-value (s^{-1})**
Au-Cu/AAO pH3	4.00×10^{-4}
Au-Cu/AAO pH5	2.00×10^{-3}
Au-Cu/AAO pH7	4.60×10^{-3}
Au-Cu/AAO pH9	6.00×10^{-4}
Au/AAO pH7 control	3.00×10^{-4}
Cu/AAO control	no reduction

Conclusion

All synthesized Au-Cu/AAOs were characterized by FESEM-EDX, FTIR, and ICP-OES. The adjustment of pH for the Au precursor during the preparation method has resulted in different Au size and arrangements. The highest activity of 4.6×10^{-3} s^{-1} was obtained for Au-Cu/AAO prepared at pH 7. Furthermore, this bimetallic catalyst exhibited higher catalytic activity than monometallic Au/AAO and Cu/AAO. Further work is underway to extend this concept by using Au NPs at pH 7 with other metals (X) to make another Au-X/AAO catalyst that can be easily recovered from liquid-phase catalytic reactions.

Acknowledgment

We would like to thank Universiti Teknologi MARA (UiTM) for providing generous internal financial support under DPPD grant: 600-TNCPI 5/3/DDN (09) (003/2020) in conducting this study and providing all the facilities.

References

1. Ahmad Zulkifli, F. W., Yazid, H. and Jani, A. M. M. (2021). Immobilization of carbon nanotubes decorated gold nanoparticles on anodized aluminium oxide (Au-CNTs-AAO) membrane for enhanced catalytic performance. *Materials Chemistry and Physics*, 264: 124445.
2. Behera, M., Tiwari, N., Basu, A., Rekha Mishra, S., Banerjee, S., Chakrabortty, S. and Tripathy, S. K. (2021). Maghemite/ZnO nanocomposites: A highly efficient, reusable and non-noble metal catalyst for reduction of 4-nitrophenol. *Advanced Powder Technology*, 32(8): 2905-2915.
3. He, R., Wang, Y.-C., Wang, X., Wang, Z., Liu, G., Zhou, W., Wen, L., Li, Q., Wang, X., Chen, X., Zeng, J. and Hou, J. G. (2014). Facile synthesis of pentacle gold–copper alloy nanocrystals and their plasmonic and catalytic properties. *Nature Communications*, 5: 1-10.
4. Heiligtag, F. J. and Niederberger, M. (2013). The fascinating world of nanoparticle research. *Materials Today*, 16: 262-271.
5. Odenbrand, C. U. I., Blanco, J., Avila, P. and Knapp, C. (1999). Lean NOx reduction in real diesel exhaust with copper and platinum titania based monolithic catalysts. *Applied Catalysis B: Environmental*, 23: 37-44.
6. Yazid, H., Adnan, R., Farrukh, M. A. and Hamid, S. A. (2011). Synthesis of Au/Al_2O_3 nanocatalyst and its application in the reduction of p-Nitrophenol. *Journal of the Chinese Chemical Society*, 58(5): 593-601.
7. Rout, L., Kumar, A., Dhaka, R. S., Reddy, G. N., Giri, S. and Dash, P. (2017). Bimetallic Au-Cu alloy nanoparticles on reduced graphene oxide support: Synthesis, catalytic activity and investigation of synergistic effect by DFT analysis. *Applied Catalysis A: General*, 538: 107-122.
8. Sobczak, I. and Wolski, Ł. (2015). Au–Cu on Nb_2O_5 and Nb/MCF supports – Surface properties and catalytic activity in glycerol and methanol oxidation. *Catalysis Today*, 254: 72-82.

9. Sharma, G., Kumar, A., Sharma, S., Naushad, M., Prakash Dwivedi, R., Al Othman, Z. A. and Mola, G. T. (2017). Novel development of nanoparticles to bimetallic nanoparticles and their composites: A review. *Journal of King Saud University-Science.* 31(2): 257-269.
10. Zeng, S., Yong, K. T., Roy, I., Dinh, X. Q., Yu, X. and Luan, F. (2011). A review on functionalized gold nanoparticles for biosensing applications. *Plasmonics*, 6(3): 491-506.
11. Rocha Rocha, M. Cortez Valadez, A. R. Hernandez Martinez, R. Gamez Cor-rales, R. A. Alvarez, R. Brito Hurtado, M. and Flores Acosta, (2019). Green synthesis of Ag-Cu nanoalloys using opuntia ficus-indica, *Journal of Electronic Material, 46*: 802-807.
12. Kumar, V., Singh, D. K., Mohan, S., Bano, D., Gundampati, R. K. and Hasan, S. H. (2017). Green synthesis of silver nanoparticle for the selective and sensitive colorimetric detection of mercury (II) ion. *Journal of Photochemistry and Photobiology B: Biology*, 168: 67-77.
13. Chen, H. J., Shao, L., Li, Q. and Wang, J. F. (2013). Gold nanorods and their plasmonic properties, *Chemical Society Reviews*, 42: 2679-2724.
14. Brust, M. and Kiely, C. J. (2002). Some recent advances in nanostructure preparation from gold and silver particles: a short topical review, *Colloids Surf. A, Physicochemical and Engineering Aspect 202* 175-186.
15. Seo, M. H., Choi, S. M., Seo, J. K., Noh, S. H., Kim, W. B., & Han, B. (2013). The graphene-supported palladium and palladium–yttrium nanoparticles for the oxygen reduction and ethanol oxidation reactions: Experimental measurement and computational validation. *Applied Catalysis B, Environmental*, 129: 163-171.
16. Habiballah, A. S., Jani, A. M. M., Mahmud, A. H., Osman, N. and Radiman, S. (2016). Facile synthesis of Ba0.5Sr0.5Co0.8Fe0.2O3-δ (BSCF) perovskite nanowires by templating from nanoporous anodic aluminium oxide membranes. *Materials Chemistry and Physics*, 177: 371-378.
17. Chung, C. K., Tsai, C. H., Hsu, C. R., Kuo, E. H., Chen, Y. and Chung, I. C. (2017). Impurity and temperature enhanced growth behaviour of anodic aluminium oxide from AA5052 Al-Mg alloy using hybrid pulse anodization at room temperature. *Corrosion Science*, 125: 40-47.
18. Nordin, N., Noor, N. M., Wahab, N. A. A., Yazid, H. and Jani, A. M. (2020). Preparation of bimetallic catalyst: gold-copper (Au-Cu) nanoparticles for catalytic reduction of p-nitrophenol. *IOP Conference Series: Materials Science and Engineering*, 957(1): 012036.